Earth Systems and Environment (2019) 3:215–230
https://doi.org/10.1007/s41748-019-00087-z

ORIGINAL ARTICLE

Simulation of Point Source Pollutant Dispersion Pattern: An Investigation of Effects of Prevailing Local Weather Conditions

Olaniran. J. Matthew[1] · Abigail N. Igbayo[1] · Felix S. Olise[2] · Kayode O. Owoade[2] · Olawale E. Abiye[3] · Muritala A. Ayoola[2] · Philip K. Hopke[4]

Received: 8 September 2018 / Accepted: 10 January 2019 / Published online: 12 March 2019

Abstract

This study investigated the potential effects of prevailing local atmospheric conditions on dispersion pattern of point source emissions from a Scrap-Iron and Steel Smelting Factory, Ile-Ife, Nigeria. The American Meteorological Society/Environmental Protection Agency Regulatory Model (AERMOD) was adopted to predict the atmospheric dispersion of particulate matter (PM) emissions around the source. The PM estimates at two experimental points (M1 and M2) around the source were compared with the observations. The model simulations suggested that the PM was mostly dispersed by the dominant southwesterly wind such that the plume moved towards the northeast with variations in their spatial distributions across the seasons. Under low wind speeds and humid conditions, there was accumulation of the pollutants within the periphery of the point source. The simulated pollutant concentrations compared fairly well with the observations for both fine PM, i.e., $PM_{2.5}$ (mean error = − 6441 µg m^{-3}, kappa coefficient, κ = 0.31 at M1 and mean error = − 16,608 µg m^{-3}, κ = 0.41 at M2) and the coarse, i.e., $PM_{2.5-10}$ (mean error = − 5506 µg m^{-3}, κ = 0.27 at M1 and mean error = − 4174 µg m^{-3}, κ = 0.36 at M2). A hypothetical increase in stack height enhanced effective plume rise which resulted in a decrease in atmospheric pollutant concentration. The study has implication in industrial air pollution reduction.

Keywords AERMOD · Particulate matter · Emission source · Dispersion · Atmospheric conditions

1 Introduction

Particulate matter (PM) is the most critical pollutant with respect to its impacts on human health and the environment. It is emitted by a wide range of man-made sources. The most significant primary sources were road transport, non-combustion industrial processes, industrial combustion plants and power generation (Cretu et al. 2010). It is usually characterized into two size fractions: fine ($PM_{2.5}$—diameter of less than 2.5 micrometers, µm) and coarse ($PM_{2.5-10}$—diameter between 2.5 and 10 µm) (Rickun 1993; Cretu et al. 2010). In the absence of precipitation, fine PM has a lifetime of multiple days in the atmosphere and it can undergo long-range transportation over hundreds of kilometers (Seigneur 2001). This is so because the particles have negligible small aerodynamic diameter and slow dry deposition rates. In the contrary, coarse particles can settle more rapidly (within hours) and normally travel only shorter distances (USEPA 2004).

The basic climatic factors affecting dispersion, chemical reaction, and deposition of pollutants are wind speed, atmospheric stability, solar radiation, precipitation, and humidity. These factors have been found to have significant effects on concentration of air pollutants in the ambient air (Qin and Oduyemi 2003; Awasthia et al. 2006; Cretu et al. 2010; Cretu and Deaconu 2012; Goudarzi et al. 2017). Other influencing factors include the physical location of the stack, nature of the terrain downwind of the stack and its characteristics (Norman 1984; Pohjola et al. 2000). Wind dilutes pollutants and rapidly disperses them throughout the immediate

✉ Olaniran. J. Matthew
abefematt@yahoo.com

[1] Institute of Ecology and Environmental Studies, Obafemi Awolowo University, Ile-Ife, Nigeria

[2] Department of Physics and Engineering Physics, Obafemi Awolowo University, Ile-Ife, Nigeria

[3] Centre for Energy Research and Development, Obafemi Awolowo University, Ile-Ife, Nigeria

[4] Department of Chemical and Bimolecular Engineering and Center for Air Resources Engineering and Science, Clarkson University, Potsdam, NY 13699-5708, USA

area. Higher wind speeds, therefore, result in lower pollutant concentrations at a given reference point. Both horizontal and vertical atmospheric motions can create turbulence near the source and this could influence dispersion of the pollutants (Pohjola et al. 2004). Atmospheric stability, which governs the vertical accelerations of the air parcel, is the single parameter used to define the turbulent state of the atmosphere or to describe the dispersion capabilities of the atmosphere (Leelossy et al. 2014). When the atmosphere is neutral or stable, the diffusion is poor and is accompanied by a lower atmospheric mixed layer, impeding the spread of pollutants and increasing the concentration (Zeng and Zhang 2017). Thus, the lower the mixing height, the lower is the volume available for the dispersion of pollutants and vice versa. Precipitation can wash out pollutant particles from the air and thereby reduce atmospheric pollutant concentration. In the contrary, humidity and precipitation can act on pollutants in the air to create more dangerous secondary pollutants, such as the substances responsible for acid rain. Similarly, solar radiation contributes to the formation of ozone and acts to create secondary pollutants in the air.

High demand for iron rods and the availability of scrap metals have led to the rapid growth of secondary iron and steel smelters in Nigeria. Unfortunately, this growth has not been matched with the necessary strict regulations for environmental and personnel protection in Nigeria. Most of these industries have not invested in the facilities necessary for improving their production processes (Otaru et al. 2013). These industries also lack installed control devices on their production processes as required. Given the wide range of pollutants associated with the production process, better understanding of the dispersion pattern of point source emissions is necessary with a view to improving our understanding of their potential impacts on the ambient air and human health (Brunekreef and Forsberg 2005).

To this end, a number of recent studies have adopted experimental method of particulate matter sampling and subsequent elemental analysis to assess atmospheric dispersion of pollutants emission from industrial facilities in Nigeria (Ezeh et al. 2012; Onwudiegwu et al. 2015; Owoade et al. 2015; Ezeh et al. 2018). However, it is not always feasible to monitor the concentrations of chemical species at various receptor sites due to high cost of the required equipment combined with the difficulties of the sampling procedure, infrastructural issues, and the availability of analytical facilities. Therefore, an efficient and less expensive way to estimate particulate matter exposures at multiple sites is the use of pollutant dispersion models, which compute atmospheric transport and dispersion of emitted pollutants. These models do not require a dense network of monitoring stations (Xie et al. 2017). In this work, therefore, the American Meteorological Society/Environmental Protection Agency Regulatory Model (AERMOD) was adopted to predict the dispersion of particulate matter emissions a Scrap-Iron and Steel Smelting Factory, Ile-Ife, Nigeria. This was with a view to assessing the practicability of the model in simulating the potential effects of prevailing local atmospheric conditions on spatial dispersion of the emissions.

2 Study Area

The Ile-Ife Iron Smelting Plant (Fig. 1) is situated along Ife–Ibadan busy highway, Osun State, Southwestern Nigeria (Fig. 2). The steel plant occupies a total of 15 hectares of land and is about 5 km away from the University campus in the Northeast direction. Ile-Ife is in the Northeast geopolitical zone of Nigeria and bound by latitude 7°28′to 7°46′ N and longitudes 4°34′ to 4°56′ E. It is situated on the elevation of between 800 and 900 feet above the sea level with prevailing tropical temperature and rainfall.

The climate of the study area is typical of equatorial rainforest being hot and humid all year round. The mean annual temperature ranges from 23 to 27 °C (AICTTRA 2012). It is dominated by two major air masses: Northeast trade wind (Harmattan wind) which prevails between November and February and the Southwest monsoon wind from the Atlantic Ocean (South monsoon wind) which is between March

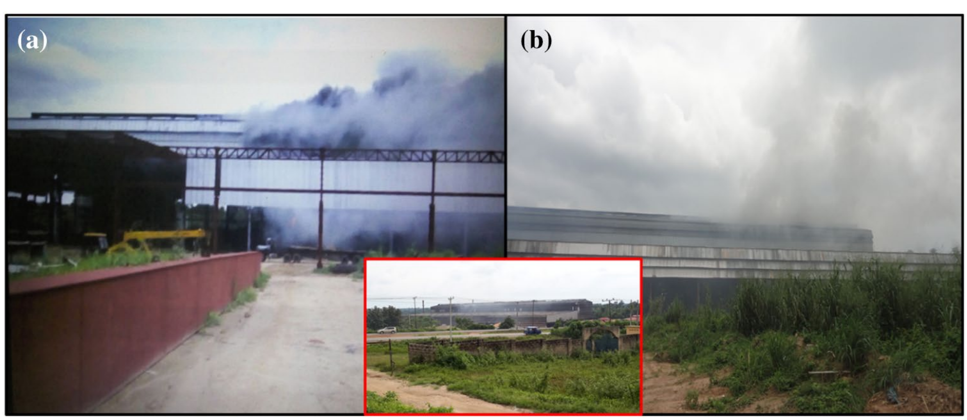

Fig. 1 Different views of the iron and steel smelting factory, Ile-Ife, southwestern Nigeria during operation (inset is the photograph of the sit at a typical idle period)

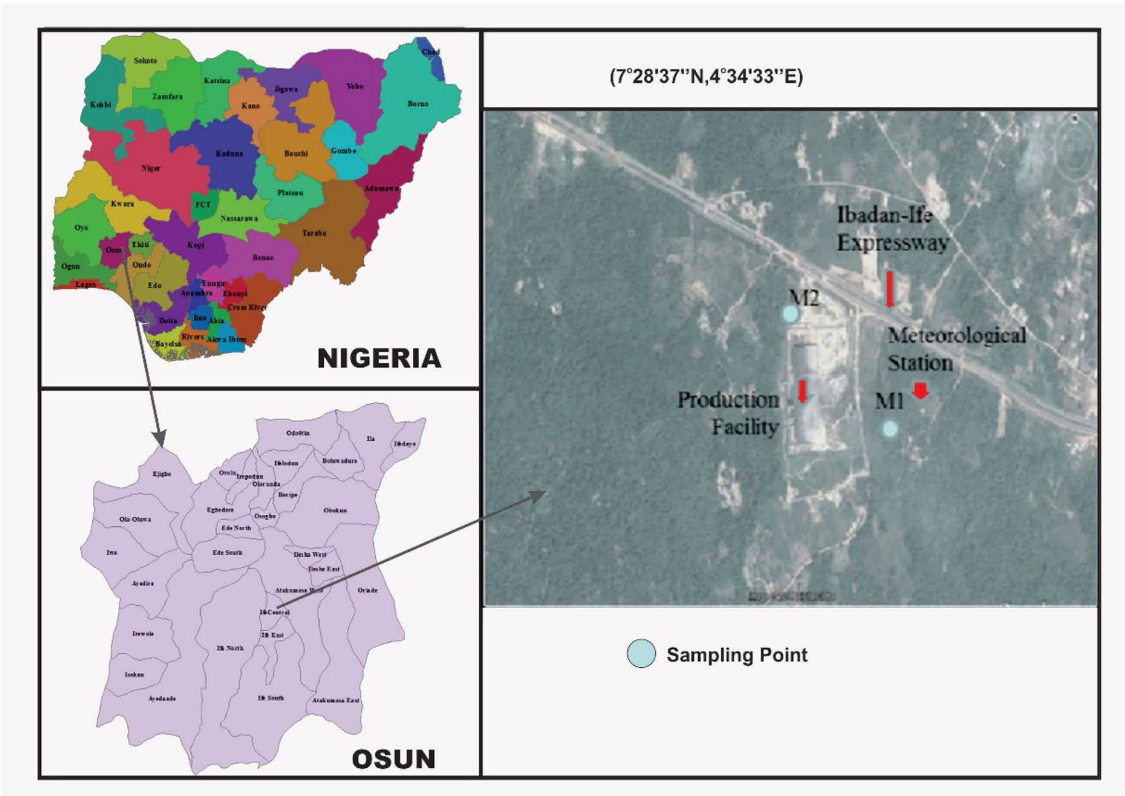

Fig. 2 Maps of study region (upper panel) in Nigeria with modeling domain (lower panel). Source: Owoade et al. (2015)

and October. There are two prominent seasons in the area: the dry and the wet (rainy) seasons. In the dry season, the temperature can be as high as above 29 °C. The daily variation of temperature is usually very small while the relative humidity is on the whole very high. The dry season lasts for about five months beginning about the late October and ending in March. The rainy season begins in the month of April and ends about the end of October. The rainfall is heavy, reaching the average of between 1143 and 1524 mm (Christiana and Amanambu 2013). Ile-Ife has an undulating terrain underlain by metamorphic rocks and characterized by two types of soils which are the deep clay soils on the upper slopes and sandy soils on the lower parts (Ajala and Olayiwola 2013). The original vegetation of Ile-Ife has been described as lowland forest zone (Muoghalu 2003) and semi-deciduous moist forests (Charter 1969; Agboola and Muoghalu 2015).

3 Methodology

3.1 Data Sources

The source characteristics at the study site were as fully described in Abiye et al. (2016a). The meteorological data (comprising ambient temperature, rainfall, relative humidity, wind speeds and directions) measured at this location were obtained from the Atmospheric Research Group, Department of Physics and Engineering Physics, Obafemi Awolowo University, Ile-Ife, Nigeria. The monthly cloud cover dataset of the Climate Research Unit, *CRU,* version TS 4.00 of the University of East Anglia, Norwich, United Kingdom (Harris et al. 2014) was also used. Other information on the point source physical characteristics such as height of stack, stack exit velocity, plume exit temperature and stack diameter was obtained during the study visit to the smelting factory. A few available primary particulate matter concentration data at two locations situated outside the steel production section but within the factory: M1 and M2 up-(westerly) and downwind (northerly) directions, respectively (Fig. 2), were obtained from an experimental data of Owoade et al. (2015).

3.2 Particulate Matter and Meteorological Data Collection

The processes involved in the collection of the particulates during the experimental work were particulate sampling and chemical analysis. The estimation of concentration of pollutants emitted into the atmosphere was carried out using the sample collection and analytical methods. Other details on materials used and methods adopted for the PM estimation have been documented by Owoade et al. (2015). The observed particulate matter emissions include both fine ($PM_{2.5}$) and coarse ($PM_{2.5–10}$) fractions. The concentrations of pollutants in the atmosphere at the source and other two points (M1-90 m east and 30 m south of the source; and M2-50 m west and 90 m north) were measured. The meteorological station sensors' descriptions and specifications have been fully reported in Abiye et al. (2016a) and Abiye et al. (2016b).

3.3 Model Simulation and Data Analyses

The dispersion model used, AERMOD, is a regulatory model approved by the US EPA for estimating the impacts of an industrial source complex on air quality in the local domain. The window-based version 12060 of the AERMOD was obtained from USEPA office (https://www.epa.gov) and adapted for estimating pollutant concentrations from the Scrap Iron and Steel Smelting Factory, Ile-Ife. It was applied for the period between May 1, 2011 and April 30, 2012. This is the period during which experimental PM data were collected. The model formulations were detailed in Cimorelli et al. (2004; 2005) and Venkatram et al. (2004). The experimental setup and model assumptions were similar to that discussed in Abiye et al. (2016a).

The instantaneous static atmospheric stability class was determined using the Pasquill stability class conditions. In this method, the wind speed and air temperature measurements at two heights ($Z_1 = 1.5$ and $Z_2 = 5.5$ m) were used to calculate the temperature gradient, $\frac{dT}{dZ}$ (Arya 2001; Manju and Siddiqui 1998):

$$\frac{dT}{dZ} = \frac{T_2 - T_1}{\sqrt{Z_2^2 + Z_1^2} \times \exp\left(\frac{Z_2}{Z_1}\right)} \tag{1}$$

Table 1 illustrates the temperature gradient limit for even stability classifications ranging from highly unstable to stable conditions.

The particulate matter emissions were simulated over an area of 500 m by 500 m around the emission source. The area covered a distance 250 m radius from the source in the east to west (x-axis) and north to south (y-axis) directions. This domain enables us to effectively capture the emission dispersion patterns around the point source in the up and downwind directions. In the simulations, it was assumed that the pollutant did not undergo chemical reactions and was not removed through any other processes including dry or wet deposition. The pollution dispersion around the industrial emission point source was investigated during the four distinct seasons, i.e, December–February (DJF), March–May (MAM), June–August (JJA), and September–November (SON) seasons. The mean emission concentrations at 0100 and 1300 h were estimated to enable the effective capture of the effects of weather patterns on the spatial dispersion under stable and unstable atmospheric conditions, respectively. The robustness of the model was evaluated by comparing the simulated concentrations at M1 and M2 with the limited number of hourly observations made during the one-year study period. The actual stack height of 20 m was used for the initial model simulations. It was replaced with hypothetical heights of 25 and 30 m (one after the other) to investigate the effects of the varying stack heights on the spatial distribution of the dispersed PM.

Comparison metrics used for the model evaluation included: correlation coefficient, mean error, Cohen's kappa coefficient of reliability, and percentage agreement. The percentage agreement, P_A, is defined as (Syed and Nelson 2015):

$$P_A = \frac{N_A}{N_A + N_D} \times 100\% \tag{2}$$

where N_A is the total number of agreements and N_D is the total number of disagreements. The Cohen's kappa coefficient, which the proportion of agreement between raters that is not due to chance, κ, is defined as (Cohen 1960; 1968; Gwet 2014):

$$\kappa = \frac{\left[N_A / \left(N_A + N_D\right)\right] - P_c}{1 - P_c} \tag{3}$$

where P_c is the index of chance agreement.

Table 1 Temperature gradient limit for stability classification (Manju and Siddiqui 1998)

Stability class group	$\frac{dt}{dz}\left(\frac{°C}{100\ m}\right)$	Stability condition
A	$\frac{dt}{dz} < -1.9$	Highly unstable
B	$-1.9 \le \frac{dt}{dz} < -1.7$	Moderately unstable
C	$-1.7 \le \frac{dt}{dz} < -1.5$	Slightly unstable
D	$-1.5 \le \frac{dt}{dz} < -0.5$	Neutral
E	$-0.5 \le \frac{dt}{dz} < 1.5$	Moderately stable
F	$1.5 \le \frac{dt}{dz} < 4.0$	Extremely stable
G	$\frac{dt}{dz} \ge 4.0$	Stable conditions

4 Results and Discussion

4.1 Observed Variations in Seasonal Weather Parameters

Figure 3 illustrates the mean monthly rainfall and relative humidity in the study area during the study period. There were two peaks of rainfall in June (260 mm) and September (320 mm). The wet season (rainfall above 150 mm per month) begins in April and ends in October. There was a drop in monthly rainfall to about 150 mm in August 2011. This period is commonly referred to as the 'August Break'. A relatively longer dry season (rainfall of 100–0 mm per month) spanned 5 months (November to March) and represents the prevailing influence of the dry and dusty northeast wind and the 'Harmattan' conditions. Relative humidity was generally high (> 50%) and relatively constant in all months. However, it was higher in the wet compared to the dry season. The monthly variation in cloud cover was very similar to the humidity with the minimum (65%) in DJF and peaked (97%) in JJA season. These results were in agreement with the results of previous studies on the climatology of the southwestern Nigeria (Odekunle 2003; Omotosho 2007). High humidity is an indication that the particles could absorb moisture from the atmosphere and becomes larger and less dispersed, resulting in high pollutant concentrations near the source.

The wind rose (Fig. 4) illustrates the observed wind speed and direction distributions during DJF, MAM, JJA, and SON. The dominant wind direction pattern in all seasons was southwest and this direction is important in the transport and dispersion of pollutants. This result is in agreement with the persistent wind direction from southwest to northeast found in the meteorological analyses of the prevailing annual wind patterns in southwestern Nigeria (Ojo 1997). The study location, in agreement with the literature (Ajayi 2010; Adaramola and Oyewola 2011; Okozi et al. 2015), was a 'low wind speed' region with maximum daily mean wind speed of less than 3 m/s in all seasons. The observed wind speed varied between 0.5 and 2.0 m/s in DJF, 1.0 and 2.0 m/s in MAM, 1.0 and 2.5 m/s in JJA and 1.0 and 2.0 m/s in SON. The highest wind speed was recorded in JJA and there was high variability in wind direction in SON season.

4.2 Atmospheric Stability Conditions

Table 2 presents the estimated mixed layer height and stability class in both day and nighttime across the seasons. Generally, the nighttime atmospheric stability condition was moderately stable over the region. During the day, however, the stability conditions were neutral in most months in DJF and in August (JJA season), but moderately stable in others. These changes could be attributed to variations in atmospheric condition due to transition from wet to dry period (Trenberth et al. 2003; Adelekan 2011; Abiye et al. 2018). Moreover, the mixed layer height had its peak (330–365 m)

Fig. 3 Observed mean monthly rainfall, cloud cover and relative humidity in the study area during the study period

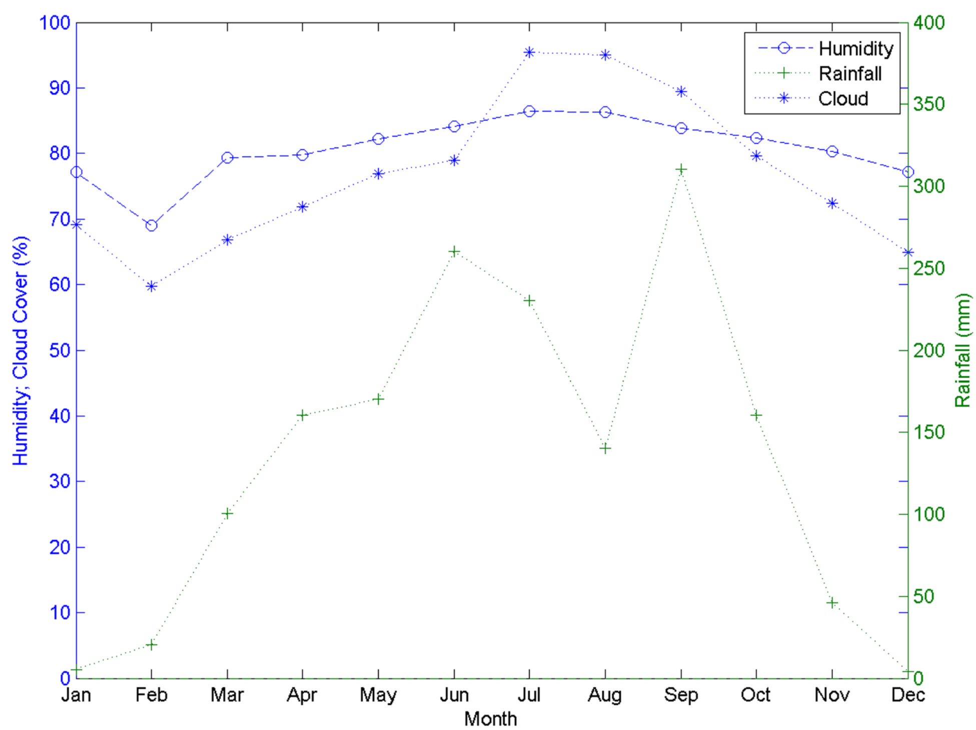

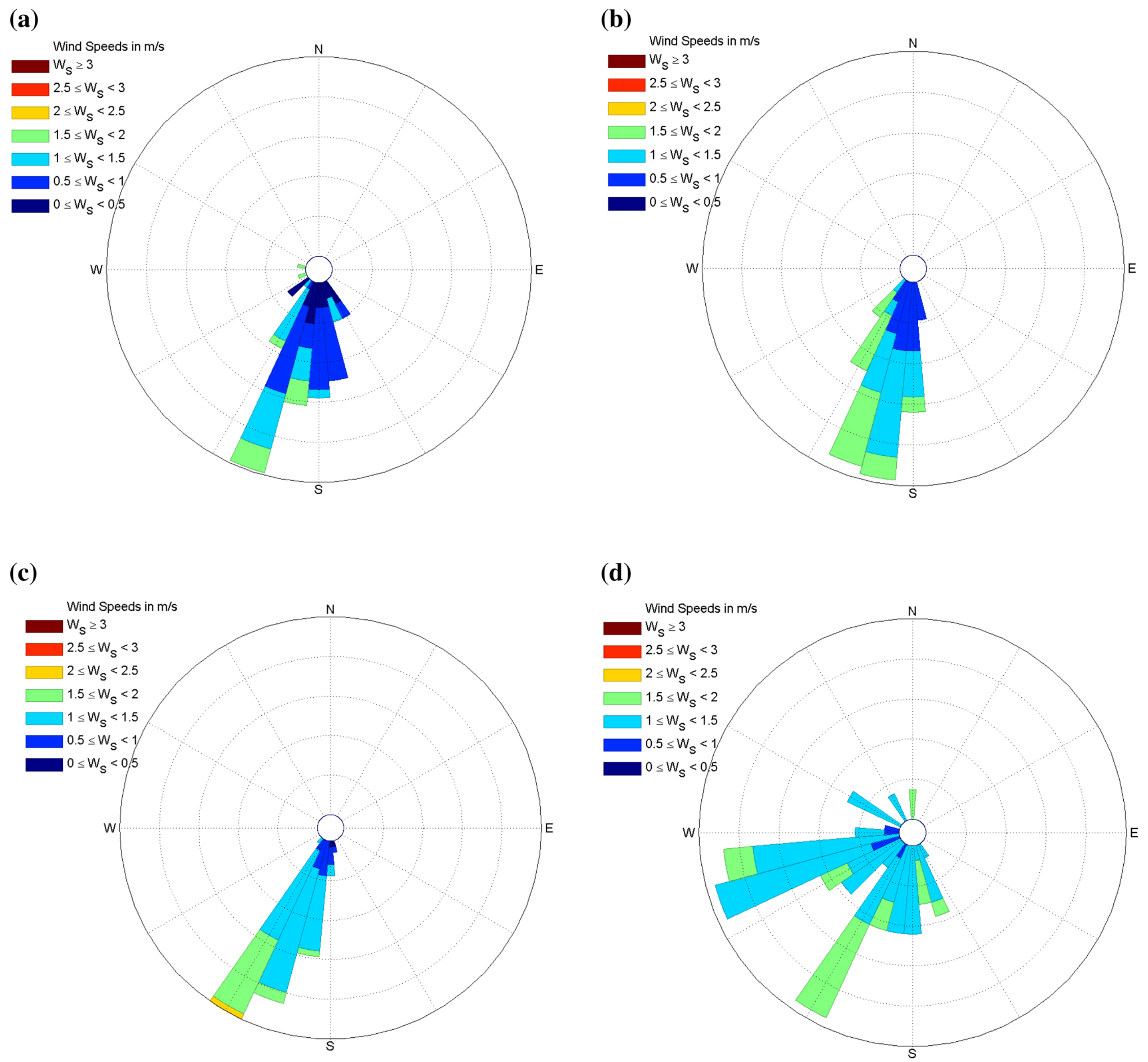

Fig. 4 Wind rose diagrams for the **a** DJF, **b** MAM, **c** JJA and **d** SON seasons

and the minimum (35–96 m) during the transitions of dry and wet seasons, respectively. It was also observed that the period of maximum mixed layer heights coincided with the dry season.

4.3 Simulated Pollutant Dispersion Pattern due to Prevailing Local Weather Conditions

Figures 5 and 6 show the spatial distribution of modeled fine and coarse PM at 0100 h (i.e., non-active production period) within 250 m radius from the source along the east to west (x-axis) and north to south (y-axis) directions during the first two (DJF and MAM) and the last two (JJA and SON) seasons, respectively. The PM concentrations increased and then decreased with increasing downwind distances from the emission source across the seasons. In DJF, for example, the maximum concentration value for fine PM was 350 μg/m^3 at 141–190 m northeast while the minimum value was 50 μg/m^3 within a 50 m radius from the source (Fig. 5a). For the coarse PM, the maximum concentration value was 450 μg/m^3 (at 141-190 m northeast), while the minimum value was 50 μg/m^3 with a 50 m radius (Fig. 5b). The patterns of

Table 2 Estimated monthly day and nighttime mean atmospheric stability conditions and the mixing height (MH) using Arya (1981) model

Season	Month	Stability class		MH (m)
		Daytime	Nighttime	
DJF	December	Moderately stable	Moderately stable	270.9
	January	Neutral	Moderately stable	176.8
	February	Neutral	Moderately stable	213.5
MAM	March	Neutral	Moderately stable	199.4
	April	Moderately stable	Moderately stable	167.7
	May	Moderately stable	Moderately stable	209.1
JJA	June	Moderately stable	Moderately stable	222.1
	July	Moderately stable	Moderately stable	175.9
	August	Neutral	Moderately stable	238.9
SON	September	Moderately stable	Moderately stable	181.0
	October	Moderately stable	Moderately stable	148.1
	November	Moderately stable	Moderately stable	262.6

distributions in MAM were similar with those obtained in DJF, but the PM concentrations were lower. In JJA and SON, the maximum concentration for fine PM was 700 μg/m^3 at 141–190 m northeast while the minimum value was 100 μg/m^3 within a 50 m radius from the source (Fig. 6). For the coarse PM, the maximum concentration was 1000 μg/m^3 (at 141–190 m northeast) while the minimum value was 100 μg/m^3 at 50 m. The PM spread was wider in SON. Pollutant concentrations decrease as the plume travels from the point of release and is dispersed by wind.

The dominant pattern of dispersal across the seasons is in the northeast direction. These observed patterns of spatial distributions of particulates are dictated by the seasonal variations in the observed prevailing wind direction and atmospheric stability as previously described by Precious et al. (2011). The highest air pollution concentrations and the largest exposed areas were found in DJF, the period of driest, least humid, and lowest wind speed conditions. Under these conditions, large quantities of emitted pollutants were transported farther in the atmosphere from the point source. The results also suggested that wet, low wind speed, and high humidity conditions hinder the vertical and horizontal diffusion of the pollutants. These conditions reduce the distance the pollutants will be transported and lead to the accumulation of the pollutants in close proximity to the point source. Similarly, the observed decrease in the particulate concentrations at further downwind distances could be ascribed to the spreading of the plume due to the influence of wind speed, interception of trees and building, deposition, and wash out (Rao et al. 2008). These findings are in agreement with the results of a study conducted by Otaru et al. (2013). In addition, wind speed and direction were found to affect the dispersion of pollutants the most. It was found that when wind speed was high in JJA, the dispersion of air pollutants was also high in the direction of the dominant wind direction (southwest). When wind speeds were lower in DJF, the dispersion of air pollutants was also reduced. This result in agreement with Khlaifi et al. (2008) is suggestive that wind speed and direction were the weather parameters that have the greatest influence on the space–time distribution of pollutants and their concentration in the atmosphere.

The spatial distribution of fine and coarse particulate matter at 1300 h (i.e., active production period) across the four seasons is depicted in Figs. 7 and 8. The patterns of dispersion were similar to those obtained during non-active production period (i.e., 0100 h) except that the dispersion pattern was narrower and the PM concentrations were much higher (1000–4000 μg/m^3) around the source in all seasons. This result was expected since the PM concentrations at any point around the source would be expected to be higher during active production hours. In addition, the pollutant dispersion was narrower due to lower mixing heights associated with the stable atmospheric condition. The wider spatial distribution of high concentrations predicted for fine PM might be attributed to the fact that their sizes are relatively smaller and they could travel farther away than coarse fractions.

4.4 Comparison of AERMOD Model simulations with the Observations

Figures 9 and 10 provide the scatter plots comparing the simulated and observed fine and coarse particulates at sampling points M1 and M2, respectively. The correlation coefficient (r), mean error ($MERR$), percentage agreement

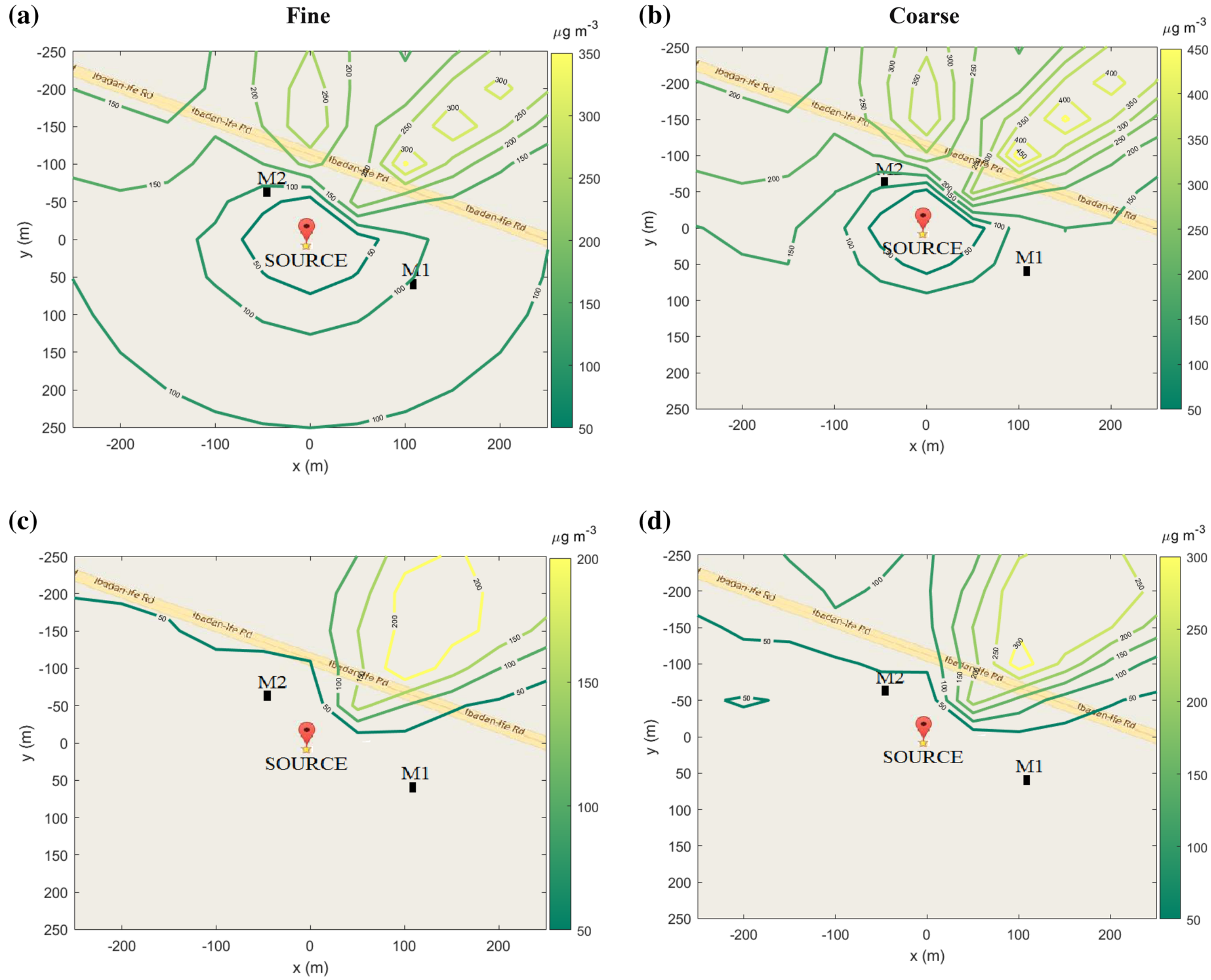

Fig. 5 Simulated spatial distribution of fine and coarse particulates (μg/m^3) at 0100 h in **a**, **b** for DJF and **c**, **d** for MAM seasons

(P_A) and kappa coefficient (κ) for the fine particulates were 0.88: 0.54, − 6441 μg/m^3:− 16,608 μg/m^3, 55.6%:50.3%, and 0.31:0.41 at M1 and M2, respectively. The r values for the coarse PM were 0.89 (at M1) and 0.94 (at M2); *MERR* were − 5506 μg/m^3 (M1) and − 4,174 μg/m^3 (M2); P_A were 65% (M1) and 58.3% (M2), while κ values were 0.27 at M1 and 0.36 at M2, respectively. The AERMOD model generally underestimated the observed PM concentrations at the two sampling points. The results suggested a fairly good comparison between the simulated and the observed pollutant concentrations when the dominant wind direction was south to north (i.e., study location upwind). In contrast to other evaluation indices (namely r, *MERR* and P_A), the estimated κ values, which accounted for agreement by chance and considered as a conservative index of reliability (Syed and Nelson 2015), were higher for the prediction of fine than coarse PM. This result suggested that the model appeared to better predict the fine PM concentrations at both points. This result was likely because the model is able to effectively capture the wide dispersion of fine PM that could travel further than the coarse particles relative to changes in environmental factors. In addition, the performance was better at M1 than at M2. The reason for this difference could be attributed to their positions upwind and their proximities relative to the source. This limited disagreement between the simulated results and the field measurements could arise primarily from the assumptions made in formulation of the predictive model (Abdulkareem et al. 2009; Piotr and Nahorski 2015) such as dry deposition on trees or other vegetation and steady-state conditions as well as other assumptions made for the estimate of the source emission rate as highlighted in Abiye et al. (2016a).

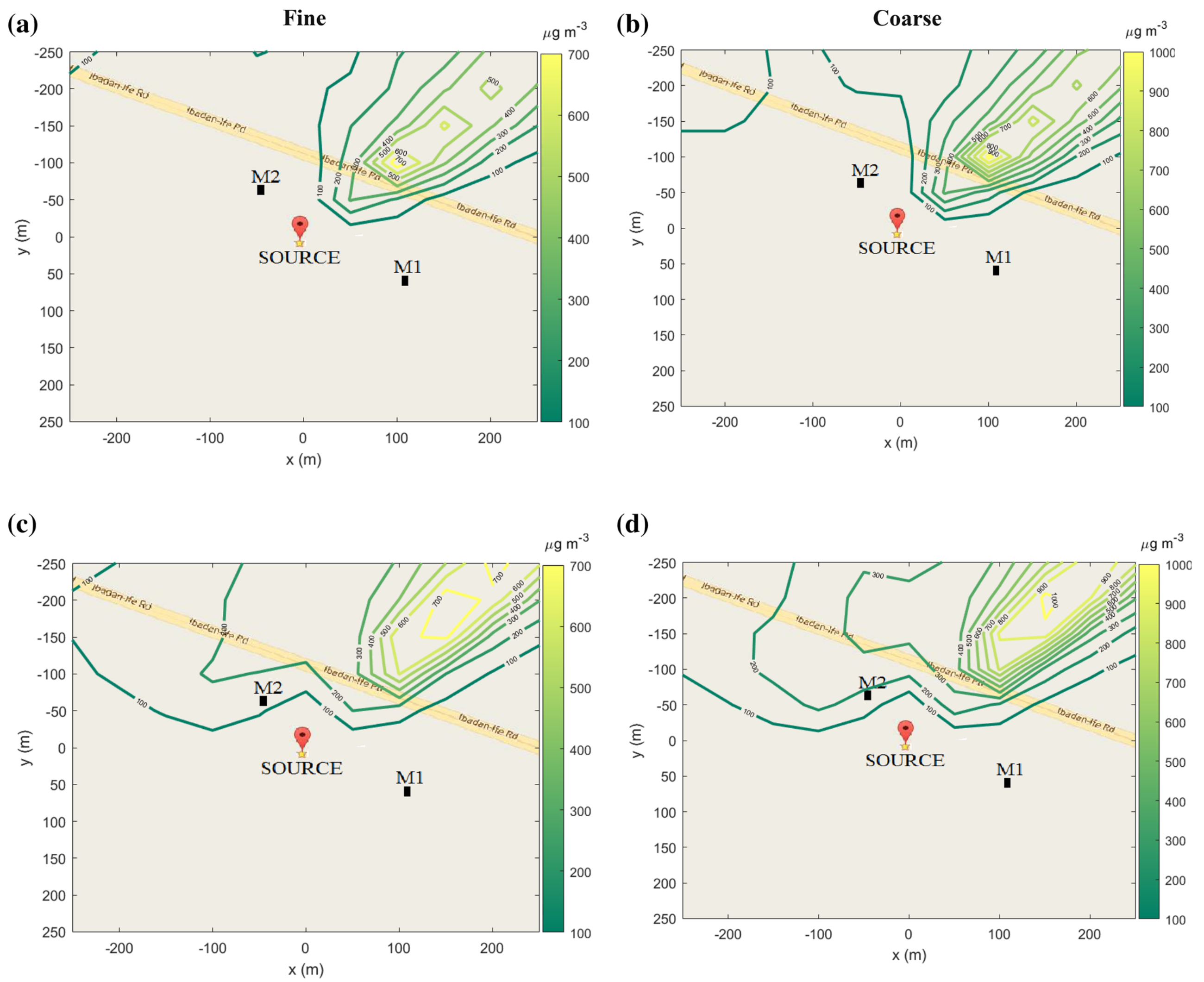

Fig. 6 Simulated spatial distribution of fine and coarse particulates (μg/m^3) at 0100 h in **a**, **b** the JJA and **c**, **d** SON seasons

4.5 Effects of Varying Stack Heights

Figure 11 illustrates the seasonal spatial distribution of fine and coarse PM for stack heights of 20, 25 and 30 m in DJF during stable atmospheric condition period (0100 h). The dominant direction pattern of PM dispersion was northeast for 20 m height stack height and radially wider spreads for the 25 and 30 m simulations. The widest dispersion was obtained with 30 m stack height for both fine and coarse PM concentrations. The maximum spatial distribution concentration values for 20, 25, and 30 m were 450 μg/m^3 (at point 150 m north and 150 m east), 160 μg/m^3 (at points 150 m south), and 100 μg/m^3 (at points 150 m south) for fine PM and 600 μg/m^3 (at 110 m north and 110 m east), 220 μg/m^3 (at points 150 m south) and 130 μg/m^3 (at points 150 m south) for the coarse. At 1300 h, the PM dispersed towards the north direction for 20 m stack as presented in Fig. 12. The dispersion patterns for 25 and 30 m stack were radially centered. The maximum concentration values for 20, 25, and 30 m were 1800 μg/m^3 (at 100 m north and 50 m east),

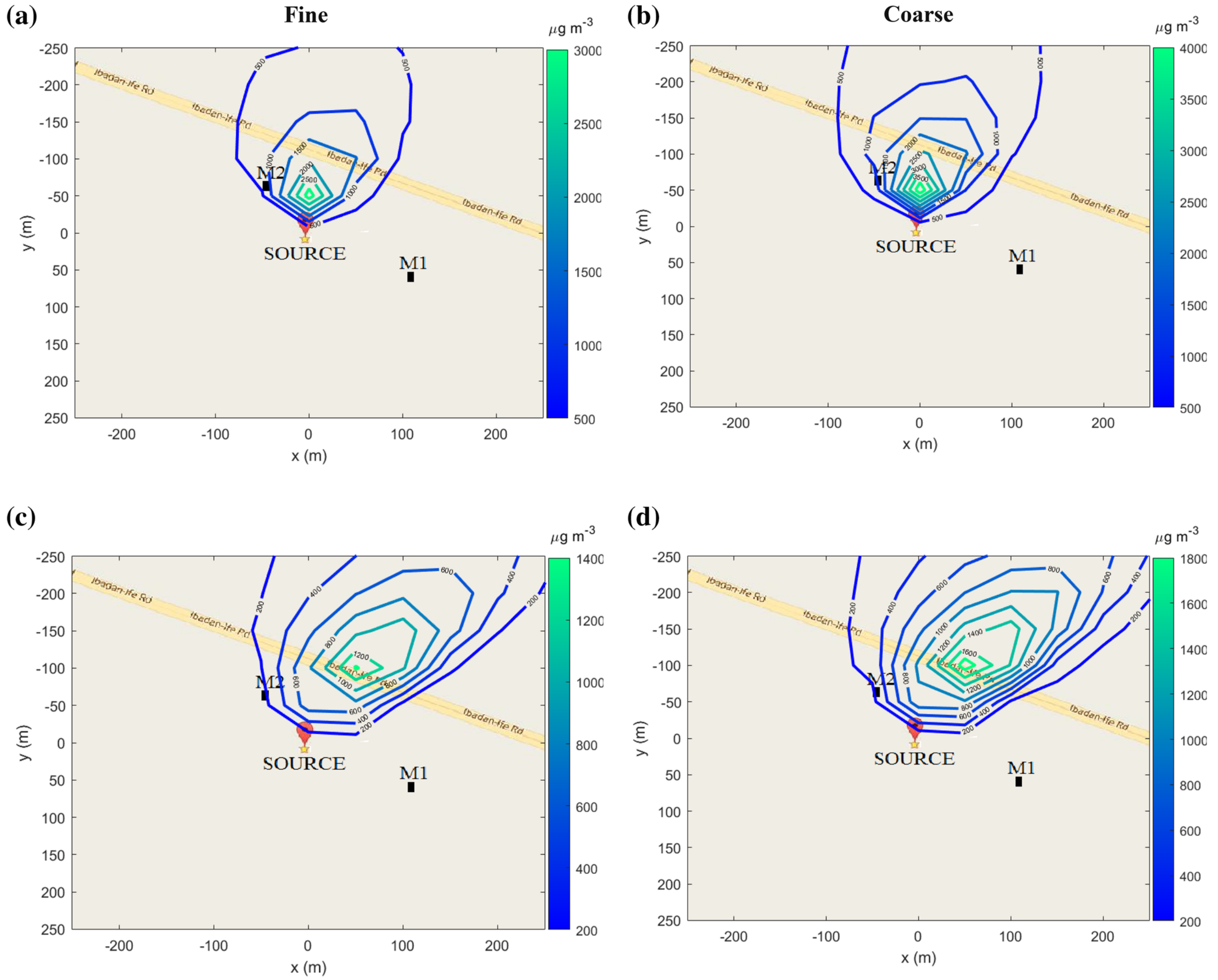

Fig. 7 Simulated spatial distribution of fine and coarse particulates (μg/m^3) at 1300 h in **a**, **b** the DJF and **c**, **d** MAM seasons

900 μg/m^3 (at 50 m north and 50 m east), and 700 μg/m^3 (at 50 m north and 50 m east) for fine PM and 2500 μg/m^3 (at 100 m north and 50 m east), 1200 μg/m^3 (at 50 m north and 50 m east) and 900 μg/m^3 (at 50 m north and 50 m east) for the coarse PM.

The maximum concentration decreased with stack height and was higher for fine than coarse PM at each height. This result indicated that varying the stack height affected ground level concentrations of the pollutants. Increased stack height was found to enhance effective plume rise resulting in a decrease in the maximum pollutant concentration with height of the stack. In agreement with the literature, an increase in the stack height enhances effective plume rise and promotes buoyancy-induced dispersion, resulting in a decrease in the maximum pollutant concentration (Ilaboya et al. 2011; Nabil and Abbas 2015). At higher stack heights, the plume will be higher in the atmosphere and the plume will, therefore, disperse more before it reaches ground level (Goudarzi et al. 2017).

5 Conclusion

The study has used the AERMOD dispersion model to simulate the dispersion of emitted particulate matter around a scrap iron and steel smelting factory located in a

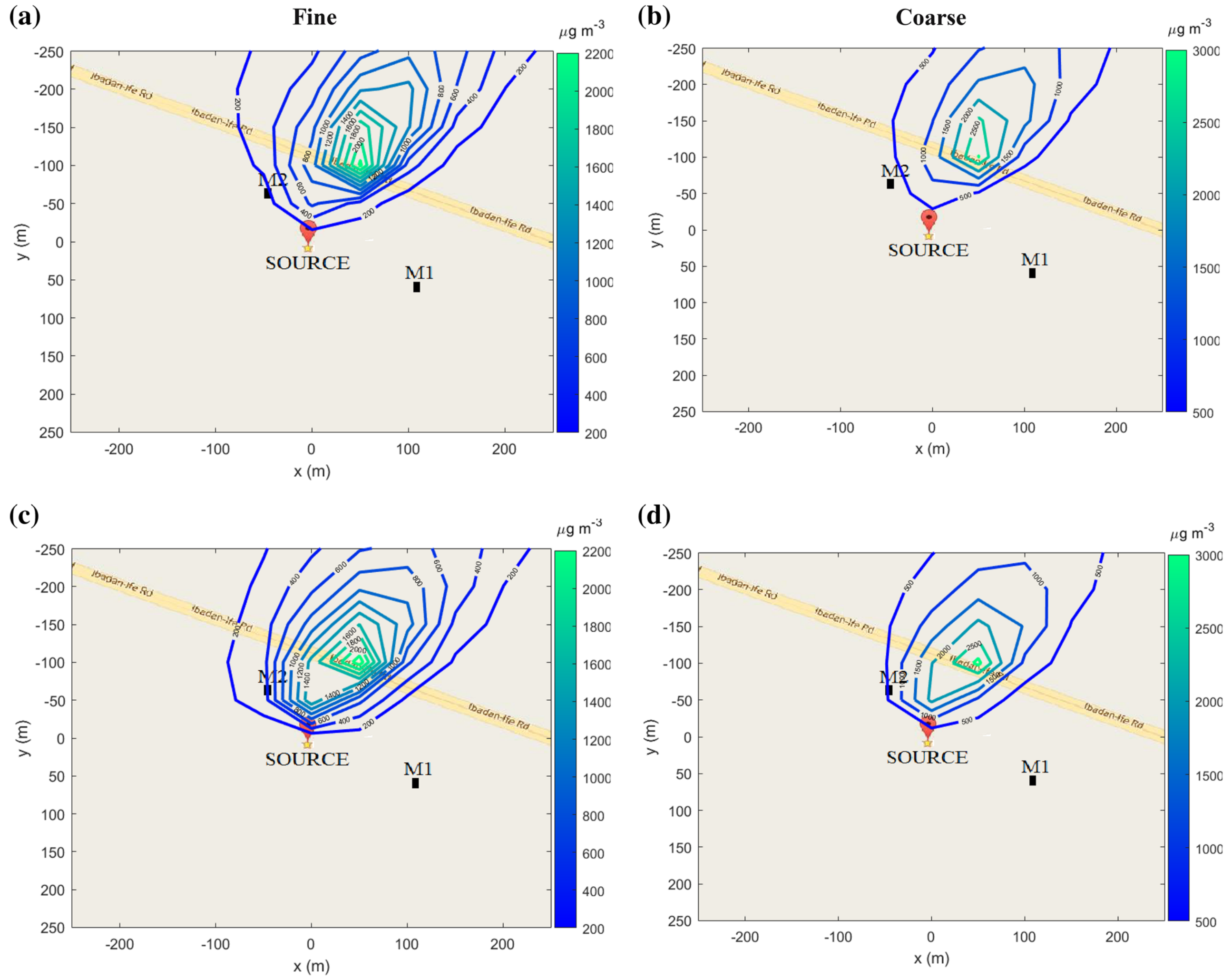

Fig. 8 Simulated spatial distribution of fine and coarse particulates (μg/m^3) at 1300 h in **a**, **b** the JJA and **c**, **d** SON seasons

tropical humid climatic region, Ile-Ife, Nigeria. It examined the effects of atmospheric conditions, and varying stack heights on the spatial distribution of the particulates and compared the model simulations with the observed pollutants at two points around the point source. To achieve these objectives, observed pollutant emission of both fine ($PM_{2.5}$) and coarse ($PM_{2.5-10}$) particulates as well as weather data collected from previously documented experimental work were used. The results revealed that AERMOD model simulations compared fairly well with the observed pollutant concentrations. The level of air pollution in the northeastern part of the smelting factory was relatively higher due to dispersion of the PM by the dominant southwesterly wind. Finally, the paper suggested that the use of stack height of 30 m or above could reduce potential negative ecological and environmental impacts of the hazardous pollutants in and around the emission source.

Fig. 9 Scatter Plots of the simulated and observed fine particulates at points **a** M1 and **b** M2, respectively (r = correlation coefficient, *MERR* = mean error, P_A = percentage agreement, and κ = Cohen's kappa coefficient)

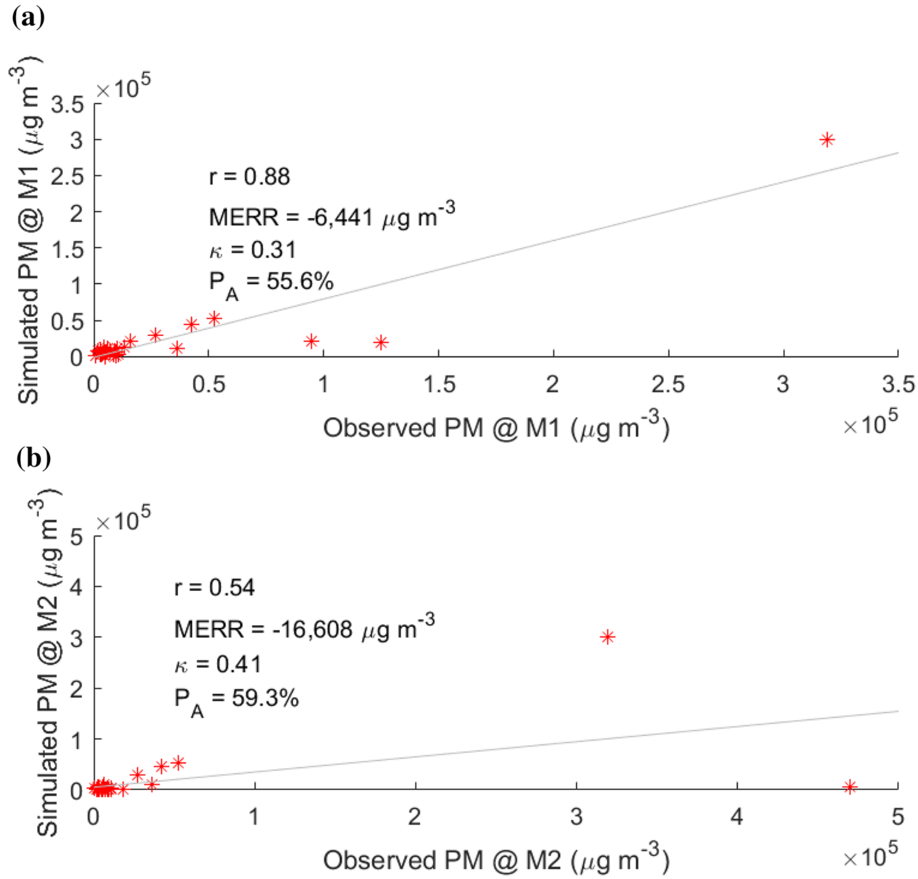

Fig. 10 Scatter plots of the simulated and observed coarse particulates at points **a** M1 and **b** M2, respectively. (r correlation coefficient, *MERR* mean error, P_A percentage agreement, and κ Cohen's kappa coefficient)

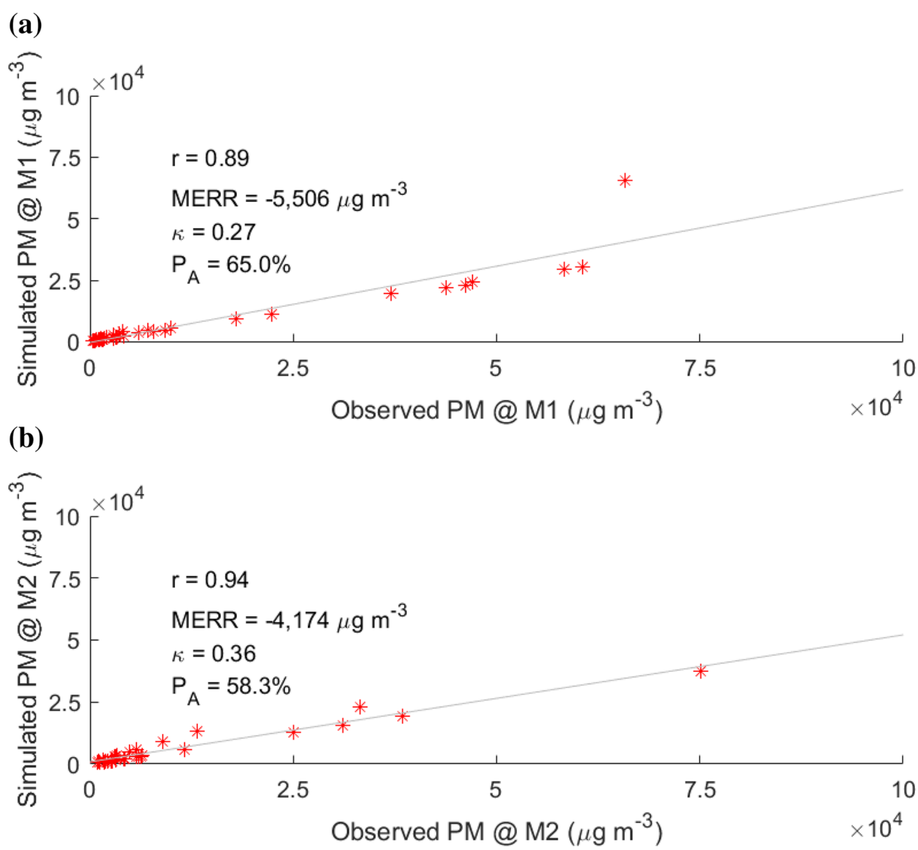

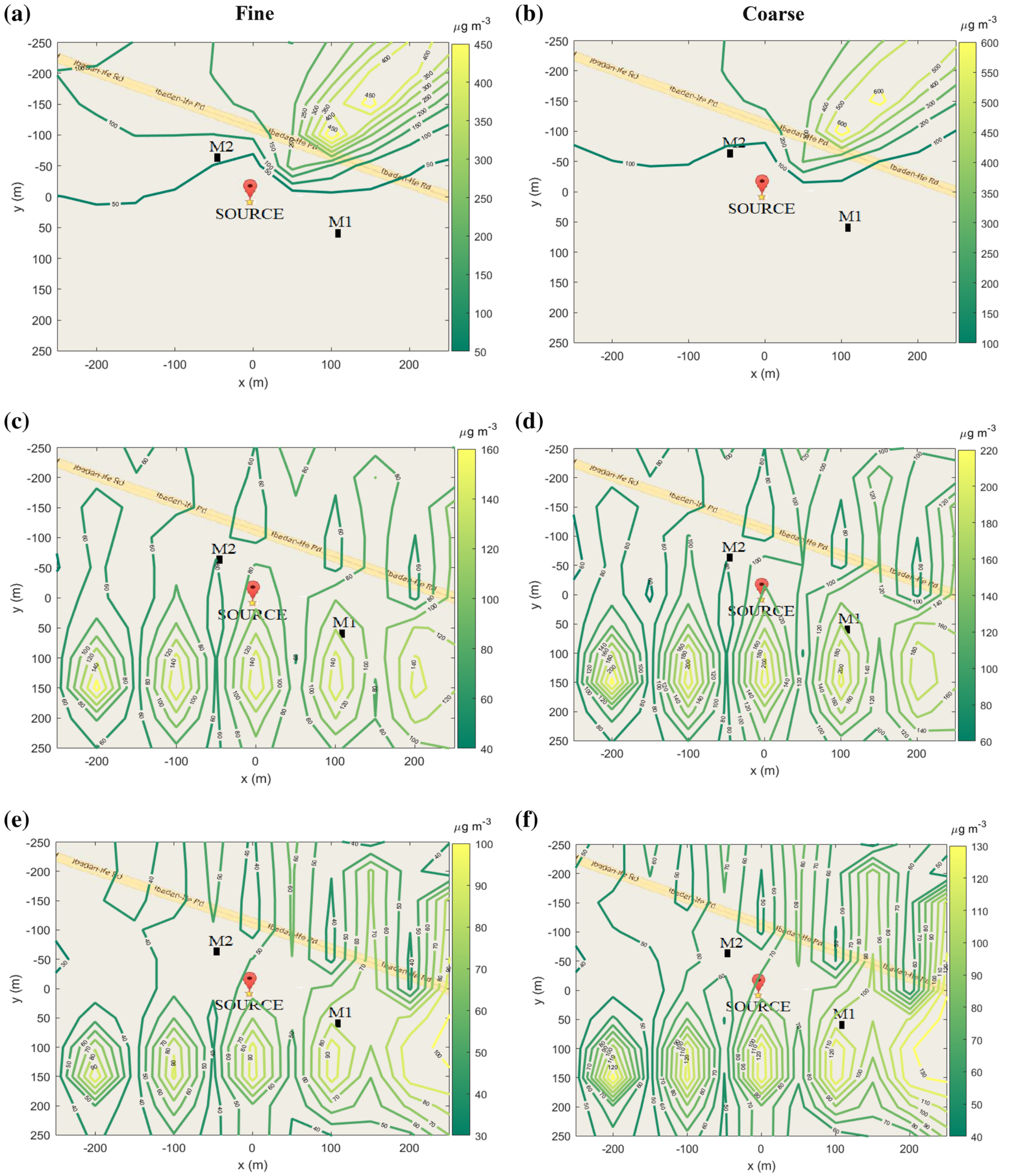

Fig. 11 Simulated spatial distribution of the seasonal mean fine and coarse particulates for stack height **a**, **b** 20 m, **c**, **d** 25 m and **e**, **f** 30 m during stable period, i.e., 0100 h

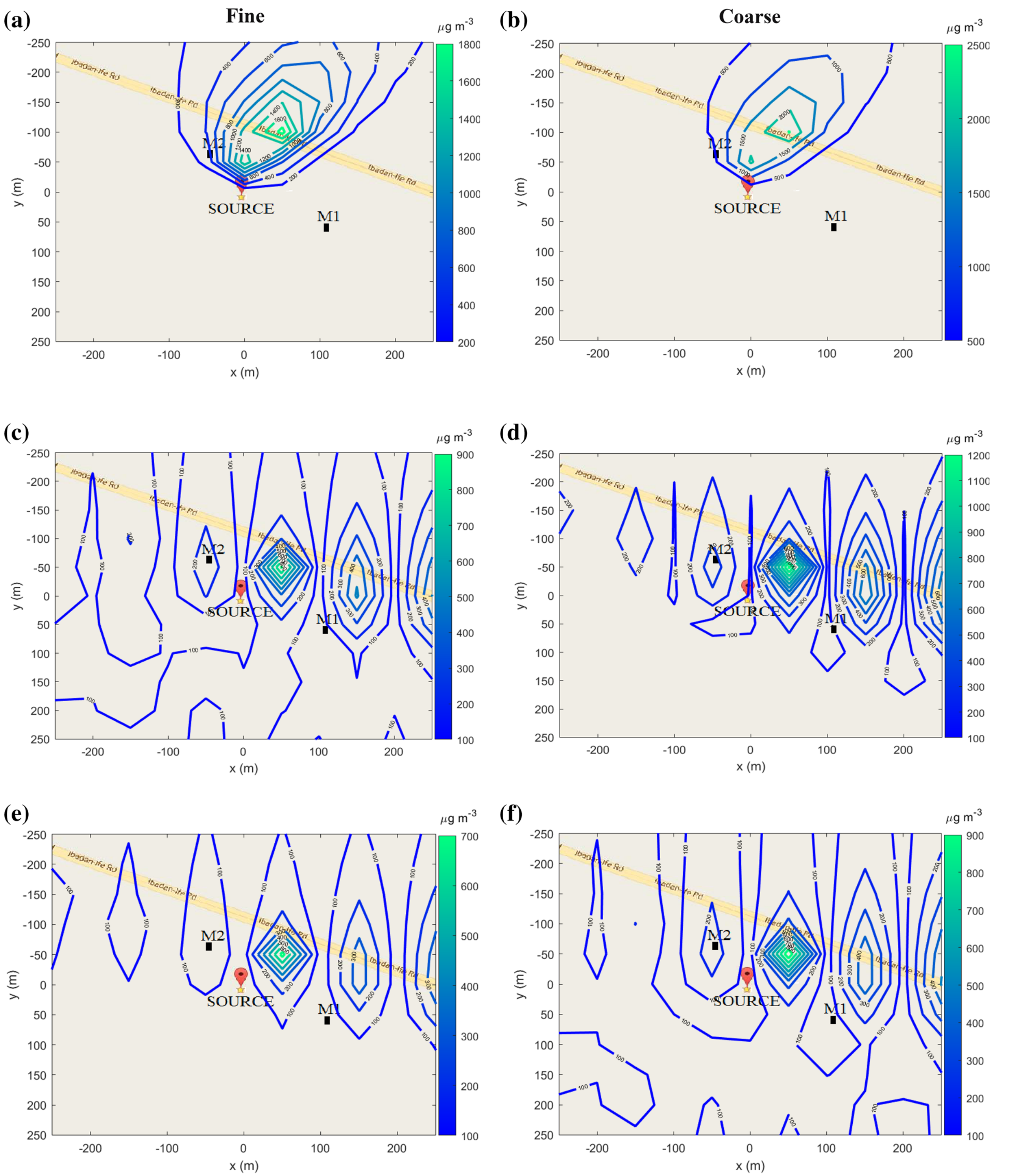

Fig. 12 Simulated spatial distribution of the seasonal mean fine and coarse particulates for stack height **a**, **b** 20 m, **c**, **d** 25 m and **e**, **f** 30 m during unstable period, i.e., 1300 h

Acknowledgements The authors are greatly indebted to the Department of Physics and Engineering Physics, Obafemi Awolowo University, Ile-Ife for providing the particulate data, point source data and the meteorological data used in this study.

Compliance with ethical standards

Conflict of interest On behalf of all authors, the corresponding author states that there is no conflict of interest. There is no financial or personal relationship with a third party whose interests could be influenced by the contents of this article.

References

Abdulkareem AS, Odigure JO, Abenege S (2009) Predictive model for pollutant dispersion from gas flaring: a case study of oil producing area of Nigeria. Energy Sources Part A 31(12):1004–1015. https://doi.org/10.1080/15567030801909318

Abiye OE, Matthew OJ, Ayoola MA, Akinola OE, Ajao AI, Babatunde OA, Sunmonu LA (2018) Potential effects of hot-buoyant air pollution plume emitted from an industrial volume source on near-source and near-surface atmospheric stability. In: Monograph of atmospheric research 2018, Centre for Atmospheric Research, Anyingba, Nigeria

Abiye OE, Sunmonu LA, Ajao AI, Akinola OE, Ayoola MA, Jegede OO (2016a) Atmospheric dispersion modeling of uncontrolled gaseous pollutants (SO_2 and NOX) emission from a scrap-iron recycling factory in Ile-Ife, Southwest Nigeria. Cogent Environ Sci 2(1):1275413. https://doi.org/10.1080/23311843.2016.1275413

Abiye OE, Akinola OF, Sunmonu LA, Ajao AI, Ayoola MA (2016b) Atmospheric ventilation corridors and coefficients for pollution plume released from an industrial facility in Ile-Ife suburb. Nigeria. Afri J Environ Sci Tech 10(10):338–349. https://doi.org/10.5897/ajest2016.2128

Adaramola MS, Oyewola OM (2011) On wind pattern and energy potential in Nigeria. Energy Policy 39(5):2501–2506. https://doi.org/10.1016/j.enpol.2011.02.016

Adelekan IO (2011) Climate change, weather extremes and society. J Environ Earth Sci 2(23):4–19

Agboola OO, Muoghalu JI (2015) Changes in species diversity, composition, growth and reproductive parameters of native vegetation invaded by chromolaena odorata and Tithonia Diversifolia in Osun State, Southwest, Nigeria. FUTA J Res Sci 11(2):217–230

AICTTRA (2012) Climate types found in Nigeria. http://www.forum.org.ng/system. Accessed 11 Jan 2013

Ajala OA, Olayiwola AM (2013) An Assessment of the growth of Ile-Ife, Osun State, Nigeria, Using Multi-Temporal Imageries. J Geol Geol. 5(2):43. https://doi.org/10.5539/jgg.v5n2p43

Ajayi OO (2010) The potential for wind energy in Nigeria. J Wind Eng 34(3):303–312. https://doi.org/10.1260/0309-524x.34.3.303

Arya F (1981) Modeling the depth of the stable boundary-layer. Boundary-Layer Meteorol 21(1):3–19

Arya SP (2001) Introduction to micrometeorology. Academic Press, San Diego, p 420

Awasthia S, Khareb M, Gargavac P (2006) General plume dispersion model (GPDM) for point source emission. Environ Modeling Assess 11:267–276. https://doi.org/10.1007/s10666-006-9041-y

Brunekreef B, Forsberg B (2005) Epidemiological evidence of effects of coarse airborne particles on health. Euro Resp J 26(2):309–318. https://doi.org/10.1183/09031936.05.00001805

Charter JR (1969) Map of ecological zones of Nigerian vegetation. Federal Department of Forestry, Ibadan

Christiana NE, Amanambu CA (2013) Climate variation assessment based on rainfall and temperature in South-Western, Nigeria. J Environ Earth Sci 3(11):2224–3216

Cimorelli AJ, Perry SG, Venkatram A, Weil JC, Paine RJ, Wilson RB, Lee RF, Peters W, Brode R, Paumier JO (2004) *AERMOD:* Description of model formulation; EPA-454/R-03-004; U.S. Environmental Protection Agency: Research Park Triangle, NC; September 2004

Cimorelli AJ, Perry SG, Venkatram A, Weil JC, Paine RJ, Wilson RB, Lee RF, Peters WD, Brode RW (2005) AERMOD: a dispersion model for industrial source applications. Part I: general model formulation and boundary layer characterization. J Appl Meteorol 44:682–693. https://doi.org/10.1175/jam2227.1

Cohen J (1960) A coefficient of reliability for nominal scales. Edu Psych Meas 20:37–46. https://doi.org/10.1177/001316446002000104

Cohen J (1968) Weighted kappa: nominal scale agreement with provision for scaled disagreement or partial credit. Psych Bull 70(4):213–220. https://doi.org/10.1037/h0026256

Cretu M, Deaconu M (2012) Air quality—monitoring and modelling. INCAS Bull 4(4):127–131. https://doi.org/10.13111/2066-8201.2012.4.4.11

Cretu M, Teleaba V, Ionescu S, Ionescu A (2010) Case study on pollution prediction through atmospheric dispersion modeling. WSEAS Environ Dev 8(6):604–613

Ezeh GC, Obioh IB, Asubiojo OI, Abiye OE (2012) PIXE characterization of PM10 and PM2.5 particulates sizes collected in Ikoyi Lagos Nigeria. Toxico Environ Chem 94(5):884–894

Ezeh GC, Ugwo JP, Adebiyi FM, Abiye OE, Onwudiegwu CA, Obiajunwa EI (2018) Proton-induced X-ray emission (PIXE) analysis of trace elements of total atmospheric deposit(TAD) around a smelting industry: aerial pollution monitor. Hum Ecol Risk Assess: Inter J 24(4):925–940. https://doi.org/10.1080/10807039.2017.1395683

Goudarzi Gh, Rashidi R, Keishams F, Moradi M, Sadeghi S, Masihpour F, Shegerd M, Mehrizi EA, Shikhrobat MV, Khaniabadi YO (2017) An assessment on dispersion of carbon monoxide from a cement factory. Environ Health Eng Manag 4(3):163–168. https://doi.org/10.15171/ehem.2017.23

Gwet KL (2014) Handbook of inter-rater reliability: The definitive guide to measuring the extent of agreement among raters, 4th edn. Advanced Analytics, Gaithersburg

Harris IC, Jones PD, Osborn TJ, Lister DH (2014) Updated high-resolution grids of monthly climatic observations-the CRU TS4.00 dataset. Int J Climatol 34:623–642

Ilaboya IR, Atikpo E, Umukoro L, Omofuma FE, Ezugwu MO (2011) Analysis of the effects of mixing height and other associated factors on the effective dispersion of plume. Ironical J Energy Environ 2(2):153–160

Khlaifi A, Dahech S, Beltrando G, Ionescua A, Candaua Y (2008) Spatial dispersion modelling of SO_2 according to the atmospheric circulation in a coastal city: sfax (Tunisia). Meteorol Appl 15:513–522. https://doi.org/10.1002/met.100

Leelossy A, Molnár F Jr, Izsák F, Havasi A, Lagzi I, Mészáros R (2014) Dispersion modeling of air pollutants in the atmosphere: a review. Central Euro J Geosci 6(3):257–278. https://doi.org/10.2478/s13533-012-0188-6

Manju M, Siddiqui TA (1998) Analysis of various schemes for the estimation of atmospheric stability classification. Atmo Environ 32(21):3775–3781. https://doi.org/10.1016/S1352-2310(98)00109-5

Muoghalu JI (2003) Contributions of throughfall, stemflow and litter fall to nutrient cycling in a secondary lowland rainforest in Ile-Ife, Nigeria. J Trop Forest Sci 15(1):339–410

Nabil HA, Abbas AA (2015) Combined influence of stack height and exit velocity on dispersion of pollutants caused by Helwan Cement Factory. Int J Comput Appl 121(9):19–24. https://doi.org/10.5120/21568-4604

Norman EB (1984) Atmospheric dispersion. Handbook of air pollution technology, Pennsylvania

Odekunle TO (2003) Rainfall and the length of the growing season in Nigeria. Int J Climatol 24(1):467–479. https://doi.org/10.1002/joc.1012

Ojo O (1997) Climates of West Africa. Heinemann, Ibadan

Okozi SO, Onyuche JC, Omeje CO (2015) Challenges facing wind energy in Nigeria. Eur J Nat Appl Sci 3(1):1–7

Omotosho JB (2007) Pre-rainy season moisture build-up and storm precipitation delivery in the West Africa Sahel. Int J Climatol 28:937–946. https://doi.org/10.1002/joc.1548

Onwudiegwu CA, Ezeh GC, Obioh IB (2015) Trace metals in total atmospheric depositions (TAD) of a Nigerian Island. J Atmosph Pollut 4(1):15–22

Otaru AJ, Odigure JO, Okafor JO, Abdulkareem AS (2013) Model prediction of particulate dispersion from a cement plant in Nigeria. IOSR J Environ Sci Toxi Food Tech 3(2):97–110. https://doi.org/10.9790/2402-0326376

Owoade KO, Hopke PK, Olise FS, Ogundele LT, Fawole OG, Olaniyi BH, Jegede OO, Ayoola MA, Bashiru MI (2015) Chemical Compositions and Source Identification of Particulate Matter ($PM_{2.5}$ and $PM_{2.5–10}$) from a scrap iron and Steel making Industry along the Ife-Ibadan highway, Nigeria. Atmo Poll Res 6(1):107–119. https://doi.org/10.5094/apr.2015.013

Piotr H, Nahorski Z (2015) Emission data uncertainty in urban air quality modeling -case study. Environ Model Assess 20:583–597. https://doi.org/10.1007/s10666-015-9445-7

Pohjola M, Kousa A, Aarnio P, Koskentalo T, Kukkonen J, Härkönen J, Karppinen A (2000) Meteorological Interpretation of Measured Urban $PM_{2.5}$ and PM_{10} Concentrations in the Helsinki Metropolitan Area. In Longhurst JWS, Brebbia CA, Power H (Eds.). Air Pollution VIII. Wessex Institute of Technology Press

Pohjola MA, Rantamäki M, Kukkonen J, Karppinen A, Berge E (2004) Meteorological evaluation of a severe air pollution episode in Helsinki on 27–29 December 1995. Boreal Environ Res 9(4):75–87

Precious NE, David OE, Oluleye A (2011) Aspect of air quality status of Benny Island, Nigeria attributed to an LNG plant. Energy Environ 221(7):892. https://doi.org/10.1260/0958-305x.22.7.891

Qin Y, Oduyemi K (2003) Chemical composition of atmospheric aerosol in Dundee, UK. Atmos Environ 37(1):93–104. https://doi.org/10.1016/s1352-2310(02)00658-1

Rao X, Li F, Zhou N, Yang K (2008) Analysis of a large-scale haze over middle and eastern China. Meteorol Mon 34:89–96 **(In Chinese)**

Rickun J (1993) Air permits, Title III, VOCs and foundries. Proceedings of the Environmental Affairs Conference. Milwaukee, WI. August 22–24

Seigneur C (2001) Current status of air quality models for particulate matter. J Air Waste Manag Associ 51(3):1508–1521. https://doi.org/10.1080/10473289.2001.10464383

Syed M, Nelson SC (2015) Guidelines for establishing reliability when coding narrative data. Emerging Adulthood 3(6):375–387. https://doi.org/10.1177/2167696815587648

Trenberth KE, Dai A, Rasmussen RM, Parsons DB (2003) The changing character of precipitation. Am Meteorol Soc 84(9):1205–1217. https://doi.org/10.1175/bams-84-9-1205

USEPA (2004) Air quality criteria for particulate matter; EPA/600/P-99/002aF; USEPA-United States Environmental Protection Agency, Washington, DC, USA

Venkatram A, Isakov V, Pankratz D, Heumann J, Yuan J (2004) The analysis of data from an urban dispersion experiment. Atmos Environ 38:3647–3659. https://doi.org/10.1016/j.atmosenv.2004.03.045

Xie X, Semanjski I, Gautama S, Tsiligianni E, Deligiannis N, Rajan RT, Pasveer F, Philips W (2017) A review of urban air pollution monitoring and exposure assessment methods. ISPRS Inter J Geo-Info 6:389. https://doi.org/10.3390/ijgi6120389

Zeng S, Zhang Y (2017) The effect of meteorological elements on continuing heavy air pollution: a case study in the Chengdu Area during the 2014 spring festival. Atmosphere 8:71. https://doi.org/10.3390/atmos8040071